PHOTO-OXIDATION OF 1,4-DIHYDROPYRIDINES BY VARIOUS ELECTRON ACCEPTORS: A LASER FLASH PHOTOLYSIS STUDY

F. M. MARTENS and J. W. VERHOEVEN

Laboratory for Organic Chemistry, University of Amsterdam, Nieuwe Achtergracht 129, 1018 WS Amsterdam (The Netherlands)

C. A. G. O. VARMA and P. BERGWERF

Gorlaeus Laboratories, University of Leiden, P.O. Box 9502, 2300 RA Leiden (The Netherlands)

(Received September 29, 1982; in revised form November 30, 1982)

Summary

The photo-oxidation of the coenzyme β-dihydronicotinamide adenine dinucleotide (NADH) and some related 1,4-dihydropyridines (PyH_2) by three electron acceptors has been studied via nanosecond laser flash photolysis.

Photo-oxidation using the potent dicationic acceptor paraquat (PQ^{2+}) is shown to be initiated by one-electron transfer from the singlet excited dihydropyridine to paraquat. This is followed by a relatively slow proton loss from the resulting dihydropyridine radical cation and consecutive rapid thermal electron transfer from the pyridinyl radical to a second molecule of PQ^{2+} thus completing an overall reaction which gives two viologen radicals ($PQ^{+\cdot}$) and one pyridinium ion (PyH^+) for each PyH_2 molecule that is oxidized:

$$PyH_2 + 2PQ^{2+} + h\nu \rightarrow PyH^+ + 2PQ^{+\cdot} + H^+$$

The same sequence is initiated with the less potent neutral electron acceptor dimethylterephthalate (DMTP), but owing to the lower reduction potential of DMTP the thermal electron transfer from the pyridinyl radical ($PyH^\cdot$) to DMTP does not occur. Photo-oxidation using the more potent neutral electron acceptor *N*,*N*′-di-*n*-pentylpyromellitic diimide is found to have the same overall stoichiometry as that using PQ^{2+}, but the mechanism is different and occurs mainly via a path involving primary hydrogen atom abstraction (probably via fast consecutive electron and proton abstraction) from the dihydropyridine by the acceptor in its lowest triplet state.

The laser photolysis data presented provide an insight into the various paths that can lead to the (photo-)oxidation of dihydropyridines. Of special interest are the quantitative data that have been obtained for the kinetic acidity of the 1,4-dihydropyridine radical cation ($PyH_2^{+\cdot}$), an elusive species

0047-2670/83/$3.00

which has been postulated as the intermediate in various thermal NADH-mediated redox processes.

---

1. Introduction

The coenzyme β-dihydronicotinamide adenine dinucleotide (3′-phosphate) (NADPH) contains the 1,4-dihydronicotinamide moiety as a chromophore and therefore a study [1, 2] of elementary (photo)chemical processes involving substituted 1,4-dihydronicotinamides may help to understand its action in (photo)biological systems.

Even molecules with moderate electron acceptor properties effectively quench the fluorescence of the 1,4-dihydronicotinamide chromophore by a mechanism [1] that obviously involves one-electron transfer. In most cases this photoinduced one-electron transfer appears to be extremely reversible and thus does not provide an efficient route towards the two-electron oxidation product, *i.e.* the nicotinamidium ion. A notable exception is the efficient photo-oxidation [2, 3] of 1,4-dihydropyridines in the presence of *N,N′*-dimethyl-4,4′-bispyridinium dichloride (paraquat (PQ^{2+})). The stoichiometry and the influence of the solvent and the irradiation wavelength on the quantum yield have been extensively discussed for the latter process in a previous publication [2].

In the work reported in this paper the stepwise nature of the photo-oxidation of several 1,4-dihydropyridines (PyH_2 in Fig. 1) by PQ^{2+} is confirmed by laser flash photolysis and this process is compared with those observed in the presence of the two non-ionic electron acceptors (A) dimethylterephthalate (DMTP) and *N,N′*-di-*n*-pentylpyromellitic diimide (PMDI) (see Fig. 1).

2. Results and discussion

2.1. Paraquat

As reported earlier [2, 3], excitation of a 1,4-dihydropyridine (PyH_2) in the presence of PQ^{2+} ($E_{1/2}^{red} = -0.69$ V (relative to the saturated calomel electrode (SCE) in CH_3CN)) leads to the formation of the paraquat radical cation ($PQ^{+\bullet}$) in a photoredox process with the overall stoichiometry

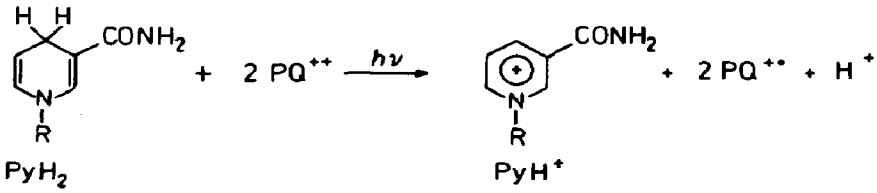

(1)

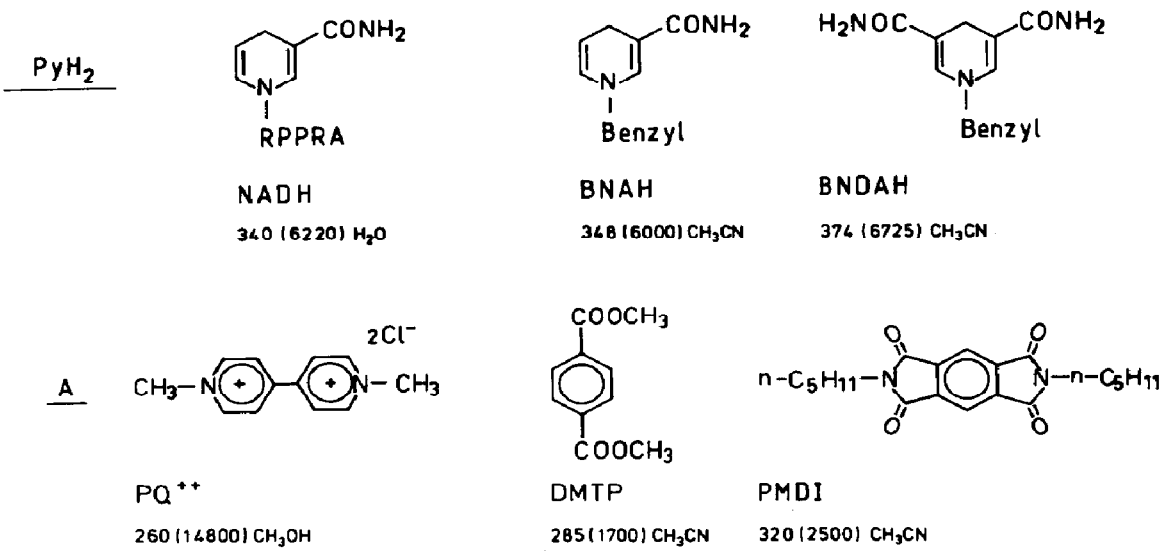

Fig. 1. Structure, abbreviated notation and absorption data (λ_{max}(nm) (ϵ_{max}(M^{-1} cm^{-1}))) for the dihydropyridines (PyH_2) and the electron acceptors (A) investigated: RPPRA, ribose–diphosphate–ribose–adenine; NADH, β-dihydronicotinamide adenine dinucleotide; BNAH, *N*-benzyl-1,4-dihydronicotinamide; BNDAH, *N*-benzyl-1,4-dihydro-3,5-dicarboxamido pyridine; PQ^{2+}, paraquat; DMTP, dimethylterephthalate; PMDI, *N,N'*-di-*n*-pentylpyromellitic diimide.

The reaction mechanism of the photoinduced oxidation of dihydropyridines by PQ^{2+} proposed earlier [2] on the basis of data obtained under conditions of continuous irradiation is shown in the following scheme:

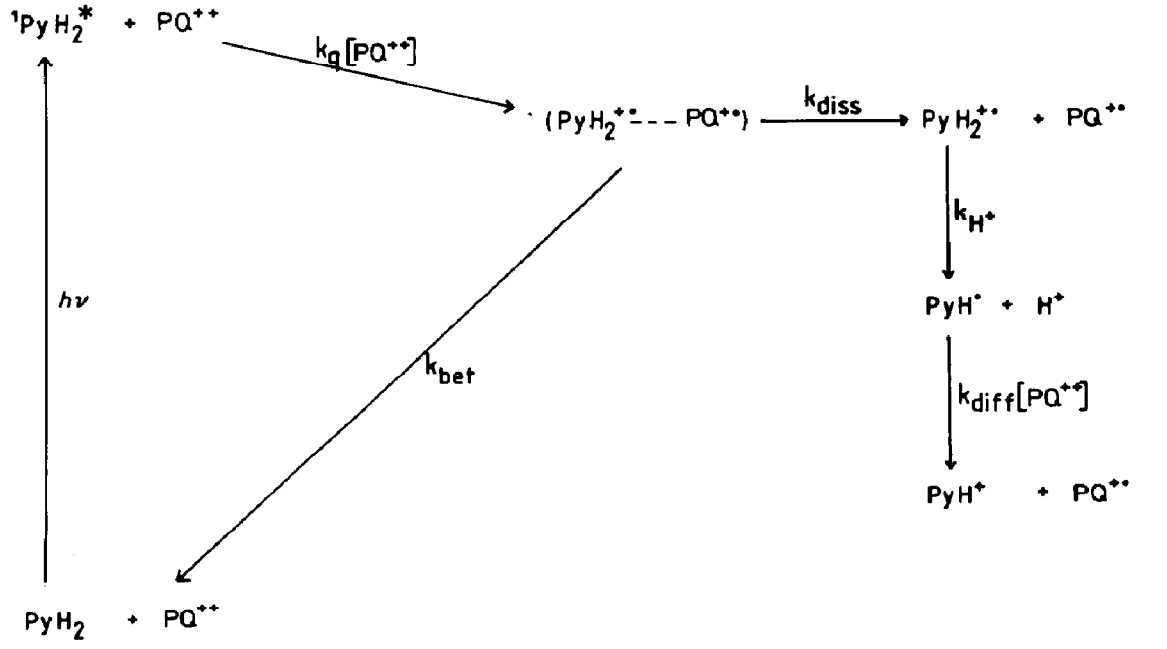

We now report the time-resolved development of the characteristic long wavelength absorption of $PQ^{+\cdot}$ (λ_{max} = 602 nm; ϵ_{max} = 12 000 (Fig. 2)) after excitation of PyH_2 in several PyH_2–PQ^{2+} mixtures by a nanosecond UV laser flash (see Section 3). (The laser flash excitation (337 nm) of concentrated aqueous PQ^{2+} solutions has been reported [4] to lead to transient $PQ^{+\cdot}$ formation as a result of light absorption by a charge transfer complex between PQ^{2+} and its chloride counter-ions. Under our conditions (347 or 353 nm (see Section 3)) no $PQ^{+\cdot}$ formation could be detected in the absence of PyH_2.)

As shown in Figs. 2 and 3 a large contribution to the ultimate optical density (detected at 650 nm to avoid interference from PyH_2 fluorescence as much as possible) is present immediately after termination of the primary excitation (full width at half-maximum (FWHM), about 20 ns). The optical density then increases slowly, except for experiments performed in the

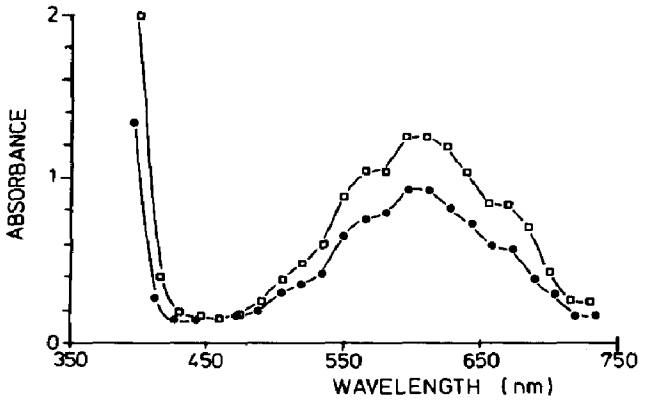

Fig. 2. Time-resolved absorption spectra of $PQ^{+\cdot}$ detected after laser flash excitation of BNAH (2×10^{-4} M) in the presence of PQ^{2+} (0.06 M) in CH_3OH: ●, 50 ns delay; □, 450 ns delay.

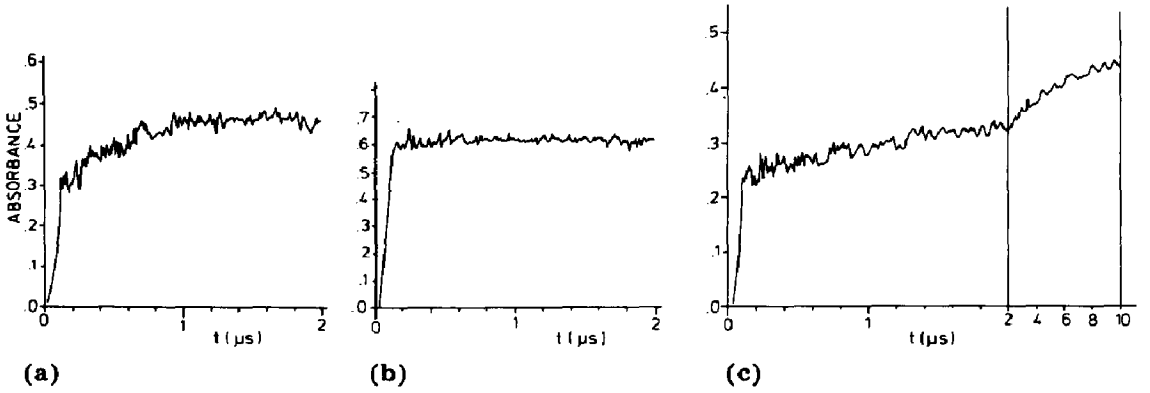

Fig. 3. Time dependence of $PQ^{+\cdot}$ absorption at 650 nm after laser flash excitation of PyH_2 (about 2×10^{-4} M) in the presence of PQ^{2+} (about 0.06 M): (a) $PyH_2 \equiv$ BNAH (solvent, CH_3OH:H_2O (1:2 by volume)); (b) $PyH_2 \equiv$ BNAH (solvent, CH_3OH:H_2O:pyridine (28:56:16 by volume)); (c) $PyH_2 \equiv$ BNAH-4d_2 (solvent CH_3OH:H_2O (1:2 by volume)).

TABLE 1

First-order rate constant k_f for the slow phase of $PQ^{+\cdot}$ formation detected at 650 nm after laser flash excitation (353 nm) of some dihydropyridines in the presence of PQ^{2+} in various solvents at 20 °C

Dihydropyridine[a]	*Solvent*	$[PQ^{2+}]$ (M)	k_f ($\times 10^6$ s^{-1})
BNAH	CH_3OH	0.01	12 ± 1
		0.02	11 ± 1
		0.06	12 ± 1
	CH_3OH:H_2O (1:2)	0.022	2.4 ± 0.1
		0.047	2.4 ± 0.1
		0.067	2.5 ± 0.1
	CH_3OH:H_2O:pyridine (28:56:16)	0.057	> 33
BNAH-4d_2	CH_3OH	0.05	2.8 ± 0.1
	CH_3OH:H_2O (1:2)	0.05	0.25 ± 0.01
		0.062	0.27 ± 0.01
NADH	H_2O	0.033	5.9 ± 0.2
	0.1 M phosphate buffer (pH 7)	0.023	12.5 ± 1
BNDAH	CH_3OH	0.03	> 33
	H_2O	0.04	14 ± 2

[a]Concentration, about 2×10^{-4} M, which gives A (1 cm) ≈ 1 at the wavelength of laser excitation.

presence of excess base (see Fig. 3(b)), over a period of several hundred nanoseconds with a time dependence that can be described using a single-exponential function. The rate constants k_f for this slow phase of $PQ^{+\cdot}$ formation are given in Table 1.

Extrapolation of the slow component of the growth curve into the laser pulse region indicates that it accounts for about 50% of the total amount of $PQ^{+\cdot}$ ultimately formed. In several cases this extrapolation cannot be made with great accuracy since substantial overlap occurs between the first part of the "slow" phase and the laser pulse. This problem is particularly acute for β-dihydronicotinamide adenine dinucleotide (NADH) and *N*-benzyl-1,4-dihydro-3,5-dicarboxamido pyridine (BNDAH) (see Table 1). In these systems the k_f values are typically in the range $k_f \geqslant 10^7$ s^{-1} which allows a large fraction of the "slow" phase of $PQ^{+\cdot}$ formation to be completed within the time domain where it cannot be followed accurately owing to both the duration of the laser pulse (FWHM, about 20 ns) and the transient deterioration of the detector response as a result of residual PyH_2 fluorescence. However, the data obtained for *N*-benzyl-1,4-dihydronicotinamide (BNAH) and BNAH-4d_2 (compare Figs. 3(a) and 3(c)) in a CH_3OH:H_2O (1:2 by volume) solvent mixture substantiate the conclusion that $PQ^{+\cdot}$ formation occurs in two phases which yield equal amounts of this species.

Whereas the fast phase appears to follow the laser pulse in all the systems studied, the rate constant k_i of the slow phase depends critically on the structure of PyH_2 as well as on the solvent system employed (see Table 1) but is independent of the PQ^{2+} concentration. In the mechanistic picture proposed in the above scheme the fast phase of $PQ^{+\cdot}$ formation can readily be attributed to the rapid ionic dissociation (k_{diss}) of an (encounter) pair with extensive charge transfer character formed (k_q) between PQ^{2+} and singlet excited PyH_2 molecules. The latter typically have a lifetime of less than 1 ns in the absence of quenchers [1, 2]. Thus the contribution of this pathway to the overall formation of $PQ^{+\cdot}$ is effectively limited to the time domain of the laser pulse. Although virtually every encounter between PQ^{2+} and a singlet excited PyH_2 molecule will lead to charge transfer and concomitant quenching of the fluorescence of the latter, ionic dissociation leading to $PQ^{+\cdot}$ will only occur in a fraction of the encounters and in the remainder back electron transfer (k_{bet}) will restore the starting materials. As shown elsewhere [2], the ratio of k_{diss} to k_{bet}, and hence the limiting quantum yield ϕ_{max} of the overall $PQ^{+\cdot}$ formation at high PQ^{2+} concentration, depends strongly on the nature of PyH_2 and of the solvent system employed. In the present systems ϕ_{max} typically ranges [2] from 0.06 for NADH in aqueous solution to 0.34 for BNAH in CH_3OH, indicating values between 0.03 and 0.17 for the ratio $k_{diss}/(k_{bet} + k_{diss})$.

The nature of the rate-limiting process in the "slow" (k_i) formation of the second half of the ultimate amount of $PQ^{+\cdot}$ molecules produced is unequivocally identified as the loss of a proton from the C(4) position of the dihydropyridines. This identification rests on (i) the lack of dependence of k_i on the PQ^{2+} concentration (see Table 1), (ii) the substantial primary isotope effect observed for this slow phase on substitution of BNAH-4d_2 for BNAH ($k_H/k_D = 4.2$ in CH_3OH and $k_H/k_D = 9.6$ in CH_3OH:H_2O (1:2 by volume) (Table 1)) and (iii) the sharp rate enhancement observed after the addition of a base (*i.e.* pyridine) as can be seen from Fig. 3 and from the data in Table 1. This rate-limiting proton loss ($k_{H^+} = k_i$) leads to the formation of neutral pyridinyl radicals ($PyH^{\cdot}$). However, these species ($\lambda_{max} \approx$ 420 nm) [5] are not detected because, owing to the large difference in redox potentials, they undergo diffusion-limited thermal electron transfer to PQ^{2+} to give PyH^+ and $PQ^{+\cdot}$ thereby completing the overall reaction (1). It is important to stress that although isotopic substitution and the addition of a base strongly influence the rate of deprotonation of $PyH_2^{+\cdot}$ they have an almost negligible influence on the ultimate amount of $PQ^{+\cdot}$ formed. (Isotopic substitution has no measurable influence (compare Fig. 3(a) with Fig. 3(c)) while pyridine slightly increases the yield of $PQ^{+\cdot}$ (see Fig. 3(b)) probably by its influence on the bulk solvent properties.) This substantiates the earlier conclusion [2] that the ratio of k_{diss} to k_{bet} is the main factor governing the quantum yield of the overall reaction.

The present observations on the rate of deprotonation of 1,4-dihydropyridine radical cations ($PyH_2^{+\cdot}$) provide a unique record of the kinetic behaviour of these elusive species even though their apparent lack of strong

absorption bands [5] in the accessible region prohibits direct observation of them. Dihydropyridine radical cations have been postulated [6 - 9] as intermediates in various (electro)chemical transformations of the NADH–NAD^+ and related redox systems. The rate constants observed for the deprotonation of $NADH^{+\cdot}$ in H_2O and in 0.1 M phosphate buffer solution (k_i values of 5.9×10^6 s^{-1} and 12.5×10^6 s^{-1} respectively (see Table 1)) agree well with a recent estimate [10] from photochemically induced dynamic nuclear polarization (photo-CIDNP) measurements on the flavin–NADH system. They deviate dramatically, however, from the value of about 60 s^{-1} at 295 K in 0.05 M phosphate buffer inferred [6] from recent studies of the electrochemical oxidation of NADH. It is clear that these latter measurements strongly underestimated the rate of proton loss and must refer to another rate-limiting electrode process such as hydride exchange between dissolved NADH and electrode-bound NAD^+. In fact the irreversible nature of the electrochemical one-electron oxidation of NADH even in cyclic voltammetry at the highest sweep rates attainable [6, 11] has been explained [11] by the assumption that proton loss from $NADH^{+\cdot}$ is fast on an electrochemical time scale!

Finally it is important to draw attention to the influence of both the solvent medium and the structure of $PyH_2^{+\cdot}$ on the rate of proton loss. The data in Table 1 consistently indicate proton loss to be faster in pure CH_3OH than in CH_3OH–H_2O mixtures or pure H_2O. It is possible that entropy effects related to changes in the hydrogen bond structure of the solvent as induced by proton translocation play a major role in the relatively slow proton acceptance by H_2O. More clear cut, however, is the response of the rate of deprotonation to changes in the pK_a difference between $PyH_2^{+\cdot}$ and the solvent. For nicotinamides a pK_a value of 1 or less has been inferred [2] for the $PyH_2^{+\cdot}$ radical cation. The introduction of a second electron-withdrawing amide group is expected to lower the pK_a even more, thereby rationalizing the faster proton loss observed for BNDAH compared with BNAH.

The dramatic increase in the rate of proton loss observed on addition of pyridine to the BNAH–PQ^{2+} system testifies to the response of this rate to the basicity of the solvent medium. This furthermore suggests that the proton (or deuteron) loss to the added bases must be considered as a very sensitive tool for the detection of $PyH_2^{+\cdot}$ as an intermediate in reactions involving transformation of the PyH_2–PyH^+ redox couple, thus enabling discrimination of stepwise one-electron transformations which involve $PyH_2^{+\cdot}$ from single-step hydride transfer transformations which do not involve this species. The extensively documented [12] absence of loss of isotopically labelled protons during enzyme-catalysed transformations of the NADPH–NADP system thus provides another compelling piece of evidence for the single-step hydride transfer mechanism in these thermal processes. Exceptions to this rule found recently [13] in non-enzymatic systems might be explicable in terms of unrecognized secondary exchange processes [12].

2.2. Dimethylterephthalate

DMTP ($E_{1/2}^{red}$ = −1.78 V (SCE) in CH_3CN) efficiently quenches the fluorescence of 1,4-dihydropyridines via a one-electron transfer mechanism [1]. Laser flash photolysis (see Fig. 4) of a CH_3CN solution containing DMTP (0.12 M) and BNAH (3×10^{-4} M) reveals the rapid development of an absorption maximum at 520 nm which is attributable to the $DMTP^{-\cdot}$ anion radical [14] followed by the much slower development of an absorption at shorter wavelengths ($\lambda_{max} \approx 420$ nm; $\epsilon_{max} \approx 1250$) which is attributed [5] to the BNA$^{\cdot}$ radical formed on slow proton loss from the $BNAH^{+\cdot}$ radical cations produced primarily by photoinduced electron transfer between excited BNAH molecules and ground state DMTP molecules. That proton loss is indeed the rate-limiting step in the production of BNA$^{\cdot}$ ($k_i \approx 1.4 \times 10^6$ s^{-1} in CH_3CN) is proved by the effect of adding a base. In the presence of pyridine (Fig. 5) both the 520 nm and the 420 nm absorption maxima develop within the duration of the laser pulse. It is clear that, owing to the

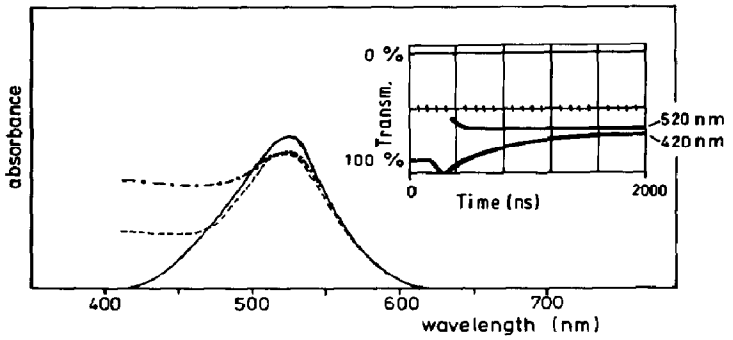

Fig. 4. Transient absorption spectra obtained after laser flash excitation (347.5 nm) of a degassed CH_3CN solution of BNAH (3×10^{-4} M) and DMTP (0.12 M): ——, directly after pulse; – – –, 500 ns after pulse; – · – ·, 1800 ns after pulse. The inset shows the time dependence of the transmissions at 420 and 520 nm.

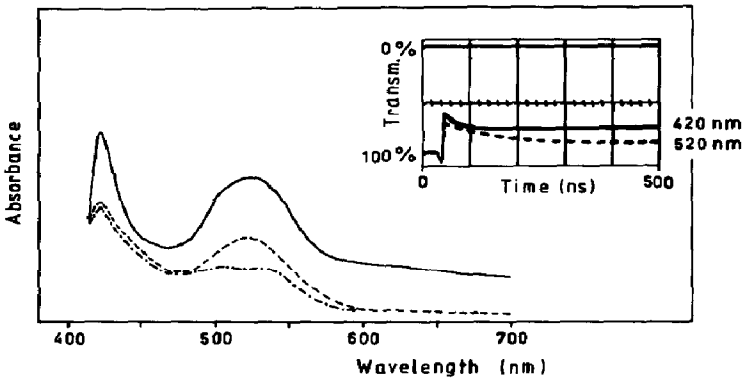

Fig. 5. Transient absorption spectra obtained after laser flash excitation (347.5 nm) of a degassed solution of BNAH (3×10^{-4} M) and DMTP (0.12 M) in CH_3CN:pyridine (85:15 by volume): ——, directly after pulse; – – –, 70 ns after pulse; – · – ·, 450 ns after pulse. The inset shows the time dependence of the transmissions at 420 and 520 nm.

weaker electron acceptor properties of DMTP compared with those of paraquat, the $BNA^{\cdot}$ radical can accumulate in the presence of DMTP without rapidly being oxidized to BNA^{+}.

The ultimate fate of both $DMTP^{-\cdot}$ and $BNA^{\cdot}$ has not been investigated in the present study. In pure degassed CH_3CN (see Fig. 4) both are stable on the maximum time scale (about 20 μs) observable during the laser flash experiments, but both decay in the presence of pyridine (see Fig. 5). Restoration of the starting materials seems implausible even in pure CH_3CN since it would require a highly endothermic reprotonation of the $BNA^{\cdot}$ radical. This process certainly cannot compete with the dimerization of the $BNA^{\cdot}$ radical which occurs [5, 15] with a rate constant k_{dim} of about 10^9 M^{-1} s^{-1} so that the dimer is one of the probable products of (prolonged) irradiation of BNAH and DMTP in pure CH_3CN. The observed instability (see Fig. 5) of both $BNA^{\cdot}$ and $DMTP^{-\cdot}$ in the presence of pyridine seems interesting in relation to the effects of pyridine on the photolytic behaviour of 1,4-dihydropyridines that have been reported previously. Thus photolysis of BNAH in the presence of pyridine has been claimed [16] to produce a species with a lifetime in excess of 60 min that is able to reduce paraquat in the dark. Other workers have denied [17] this claim but have reported strongly enhanced yields for the photoinduced reduction of diethyl fumarate and related electron-deficient ethylenic species by BNAH in a pyridine solvent compared with the yields in a CH_3CN solvent. As shown by the present studies the nature of the reactive species produced in these processes still requires clarification.

2.3. N,N'-di-n-pentylpyromellitic diimide

The efficiency of paraquat and related bipyridinium cations as electron acceptors in the photo-oxidation of PyH_2 is a consequence of (i) efficient ionic dissociation of the excited encounter complex ($PyH_2^{*}\ldots PQ^{2+}$) and (ii) irreversible oxidation of the pyridinyl radical ($PyH^{\cdot}$), obtained after proton loss from $PyH_2^{+\cdot}$, by thermal electron transfer to PQ^{2+}.

The charge separation after electron transfer in the encounter complex with PQ^{2+} is probably augmented [2] by Coulomb repulsion between the resulting positively charged species, an effect which is not available to systems containing a neutral species as an acceptor. The thermal oxidation of $PyH^{\cdot}$ only requires a sufficiently low reduction potential of the acceptor compared with that of PyH^{+} (for BNA^{+} $E_{1/2}^{red} = -0.97$ V (SCE) in CH_3CN). However, in practice selection of sufficiently strong neutral electron acceptors (*e.g.* quinones or polynitroaromatics) is limited owing to their rapid thermal reactions with PyH_2. Most of these reactions appear to proceed by direct hydride transfer [1].

PMDI ($E_{1/2}^{red} = -0.88$ V (SCE) in CH_3CN) was found to be unreactive towards BNAH in the dark. Nevertheless there is another complication involving partial overlap of the absorption spectra of BNAH and PMDI at the laser frequency (Fig. 6). Stationary photolysis of deoxygenated BNAH–PMDI solutions in CH_3CN at 365 nm leads to the formation of the green

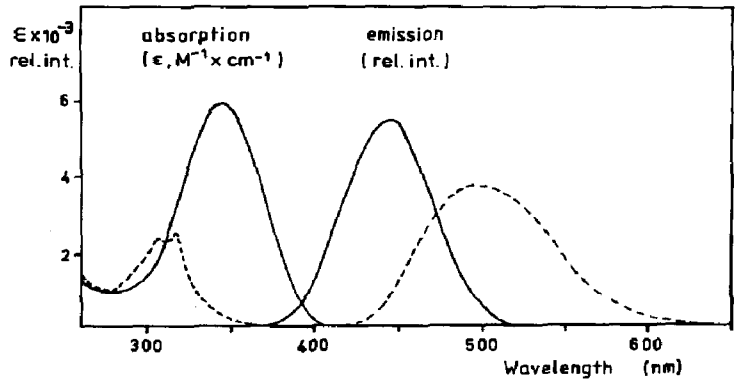

Fig. 6. Absorption and fluorescence of BNAH in CH_3CN (——) and absorption (in CH_3CN) and phosphorescence (in a polymethylmethacrylate matrix) of PMDI (– – –).

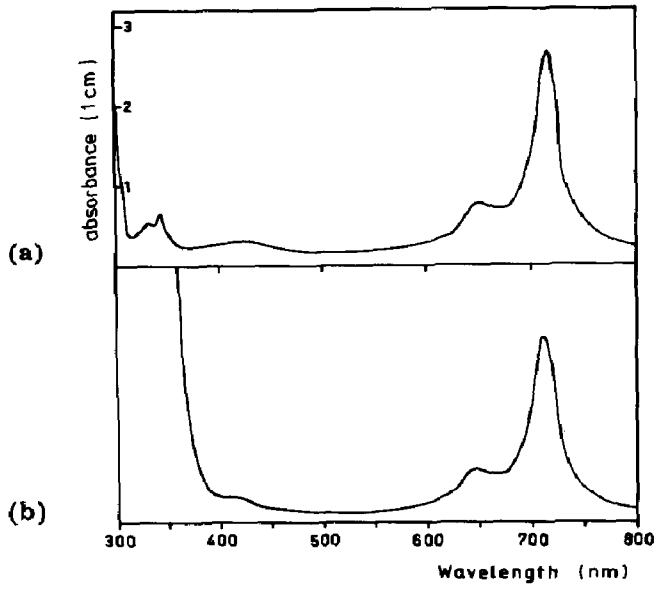

Fig. 7. Absorption spectra of (a) an irradiated solution of BNAH and PMDI (5.5×10^{-4} M) in CH_3CN and (b) a PMDI solution (1×10^{-4} M) in CH_3CN after treatment with sodium amalgam.

$PMDI^{-\cdot}$ radical anion. The radical anion thus prepared is stable for a period of about 1 week and has been identified by comparing its visible absorption with that obtained when PMDI is reduced with sodium amalgam (Fig. 7).

Stationary photolysis shows that approximately 2 mol $PMDI^{-\cdot}$ are produced for every mole of BNAH consumed:

$$BNAH + 2PMDI + h\nu \rightarrow BNA^{+} + 2PMDI^{-\cdot} \quad (2)$$

Although this stoichiometry is similar to that found with paraquat as an acceptor (reaction (1)), flash photolysis reveals the very different nature of the processes involved.

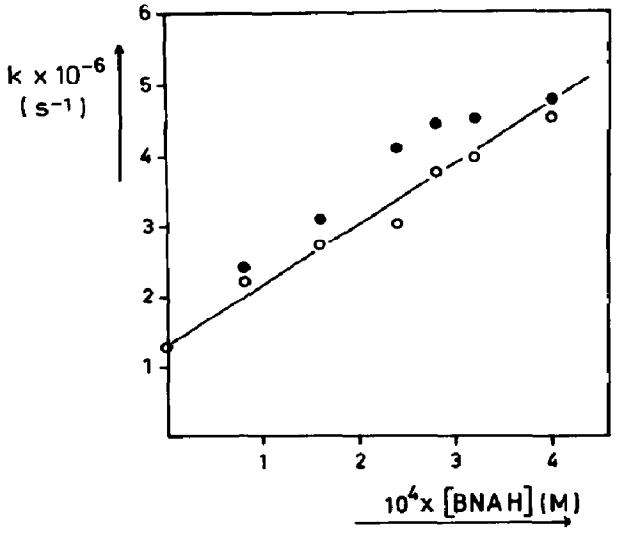

Fig. 8. Pseudo-first-order rate constants for the decay of ^{3}PMDI* (monitored at 555 nm) and the growth of PMDI$^{-\cdot}$ (monitored at 720 nm) after laser flash excitation of deoxygenated CH_3CN solutions of PMDI (4×10^{-3} M) containing various BNAH concentrations: ○, k_{555}; ●, k_{720}.

A transient species displaying strong absorption maxima at 420, 510 and 555 nm is formed during the laser flash. This species decays monoexponentially (as monitored at 555 nm) with a rate constant k_{555} that depends linearly on the BNAH concentration (Fig. 8). At the same time the characteristic 720 nm absorption of PMDI$^{-\cdot}$ develops with a rate constant k_{720} that is equal to k_{555} within the limits of experimental uncertainty (see Fig. 8). The transient species is identified as the lowest triplet of PMDI (^{3}PMDI*) by comparison with the absorption spectrum of ^{3}PMDI* observed after excitation of PMDI in a polymethylmethacrylate matrix. Under the latter conditions ^{3}PMDI* shows strong phosphorescence [18] (see Fig. 6) with a lifetime of approximately 10 ms. Excitation of PMDI in CH_3CN solution in the absence of BNAH leads to transient ^{3}PMDI* absorptions (Fig. 9) with decay rate constants k_D of 1.28×10^6 s^{-1} and 1.7×10^6 s^{-1} under deoxygenated and aerated conditions respectively. Addition of 0.03 M of the triplet quencher 3,3,4,4-tetramethyldiazetine dioxide (TMDD) leads to complete quenching of ^{3}PMDI* [19].

From the data compiled in Fig. 8 the following equations are found to describe the time dependence of the ^{3}PMDI* and PMDI$^{-\cdot}$ concentrations after laser flash excitation in degassed CH_3CN solutions containing both PMDI and BNAH:

$$[^3\text{PMDI}^*]_t = [^3\text{PMDI}^*]_0 \exp(-k_D - k_R[\text{BNAH}])\, t \quad (3)$$

$$[\text{PMDI}^{-\cdot}]_t = [\text{PMDI}^{-\cdot}]_\infty \{1 - \exp(-k_D - k_R[\text{BNAH}])\, t\} \quad (4)$$

where k_D represents the decay rate constant of ^{3}PMDI* in the absence of BNAH ($k_D = 1.28 \times 10^6$ s^{-1}) and k_R represents a second-order rate constant

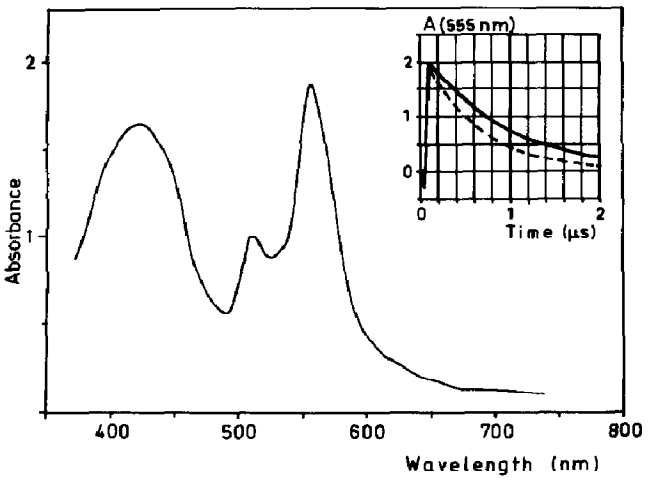

Fig. 9. Laser-flash-induced absorption (353 nm) of PMDI (0.004 M in CH_3CN solution). The inset shows the decay of the optical density at 555 nm for an aerated (– – –) and a deoxygenated (———) solution.

for which a best fit to the experimental data is obtained with a value k_R of $8.7 \times 10^9\ M^{-1}\ s^{-1}$.

These results show that ^{3}PMDI* is the main photoactive species even though most of the exciting light is absorbed by BNAH. Apparently the quantum yield for production of $PMDI^{-\cdot}$ via a pathway involving the reaction of ^{1}BNAH* with PMDI, analogous to the reaction with PQ^{2+}, is very low. A minor contribution of such a pathway to the overall $PMDI^{-\cdot}$ formation may be indicated by the observation that the addition of TMDD (0.03 M), which quenches ^{3}PMDI* completely, reduces the formation of $PMDI^{-\cdot}$ to about 10% of the amount produced in the absence of TMDD.

The value of k_R indicates that the rate-limiting step in the formation of $PMDI^{-\cdot}$ consists of a nearly diffusion-limited reaction between ^{3}PMDI* and BNAH. Since k_R was found to be unchanged by substitution of BNAH-4d_2 for BNAH, it is tempting to suggest that one-electron transfer between ^{3}PMDI* and BNAH forms the rate-limiting process

$$^3\text{PMDI}^* + \text{PyH}_2 \rightarrow \text{PMDI}^{-\cdot} + \text{PyH}_2^{+\cdot} \qquad v_5 = k_R[\text{PyH}_2] \tag{5}$$

followed by proton loss

$$\text{PyH}_2^{+\cdot} \rightarrow \text{PyH}^{\cdot} + \text{H}^+ \qquad v_6 = k_{\text{H}^+} \tag{6}$$

and thermal-diffusion-limited electron transfer

$$\text{PyH}^{\cdot} + \text{PMDI} \rightarrow \text{PyH}^+ + \text{PMDI}^{-\cdot} \qquad v_7 = k_{\text{diff}}[\text{PMDI}] \tag{7}$$

thus completing the oxidation of BNAH to BNA^+ (reaction (2)).

The concentration range of BNAH studied is limited to $[BNAH] \leqslant 4 \times 10^{-4}$ M, since at higher concentrations there is insufficient penetration of the laser light into the sample cell. Within this range the rate of reaction (5) may indeed be expected to be lower than ($v_5 = k_R[BNAH] \leqslant 3.56 \times 10^6\ s^{-1}$) or

comparable with v_6 if the latter is assumed to be equal to the $k_{H^+} = k_I$ value estimated for the photoreaction of BNAH with PQ^{2+}, albeit in different solvent systems (see Table 1). With BNAH-4d_2, however, v_6 might be expected to be sufficiently lower than v_5 to introduce a detectable isotope effect on the overall rate of formation of $PMDI^{-\cdot}$. As noted above such an effect is not observed. This may indicate that $PMDI^{-\cdot}$ plays an active role in mediating proton transfer from $PyH_2^{+\cdot}$ to the solvent. In fact it has been suggested earlier [20] that the triplet excited state of cyclic aromatic imides abstracts the equivalent of a hydrogen atom from electron-rich molecules via rapid consecutive electron and proton transfer. Such a mechanism for hydrogen abstraction from tertiary amines by triplet benzophenone has recently been observed by picosecond flash photolysis [21]. In conclusion the photooxidation of BNAH by PMDI, although stoichiometrically related to that by PQ^{2+}, occurs mainly via a triplet mechanism involving ^{3}PMDI* and only to a small extent via a singlet mechanism involving ^{1}BNAH*. The relatively high efficiency of charge separation via the triplet mechanism can be attributed to the low tendency of the triplet radical ion pair formed on electron transfer from BNAH to ^{3}PMDI* to revert to the ground state molecules via back electron transfer and concomitant spin inversion. The tendency of back electron transfer is probably much higher for the singlet radical ion pair formed on electron transfer from ^{1}BNAH* to PMDI and furthermore ionic dissociation of this singlet ion pair is not augmented by Coulomb repulsion as it is when PQ^{2+} is the acceptor.

3. Experimental details

3.1. Materials

BNAH and BNAH-4d_2 were synthesized according to standard procedures [22]. BNDAH was prepared by an analogous method to that used for other 3,5-disubstituted 1,4-dihydropyridines [23]. PMDI was synthesized and purified as described in ref. 24. All other compounds and solvents were of the highest grade of purity commercially available.

3.2. Instrumentation

Details of the stationary photolysis experiments and of quantum yield determinations have been given elsewhere [2].

A Cary 17D spectrometer and a Spex-Fluorolog spectrometer were used to record the absorption spectra and emission spectra respectively. The emission spectrometer was provided with a xenon flashlamp which allowed phosphorescence lifetime measurements to be made.

The electrochemical reduction potentials were measured at a dropping mercury electrode in a CH_3CN solvent using a Metrohm polarograph. Tetraethylammonium perchlorate was used as the supporting electrolyte. Most of the flash photolysis experiments were performed using primary excitation at the third-harmonic frequency of a *Q*-switched Nd^{3+} glass

laser, *i.e.* at 353 nm. The total excitation energy at 353 nm was about 10 mJ. The analysing light from a pulsed Osram XBO-450 xenon lamp passed through a monochromator, the sample (path length, 1 cm perpendicular to the laser beam) and a second monochromator before being detected by an RCA 4840 photomultiplier which was wired for fast response and linearity at high peak intensities. The analysing light pulse had a constant peak intensity over a period of 200 μs during which the primary excitation was deposited in the sample. The transient photomultiplier signals were fed into a Tektronix R 7912 transient digitizer and were then stored in a PDP 11/10 computer. The transient optical densities were calculated using the peak intensity of the analysing light and were then normalized with respect to the total primary excitation energy. The curves through the normalized optical densities were recorded using a Tektronix 4662 plotter.

Some of the flash photolysis experiments, mainly those with DMTP as the acceptor, were performed using less sophisticated equipment [25] but with higher total primary excitation energy per pulse and with a double-pulsed analysing xenon flash for better suppression of fluorescence, thus enabling detection of transients formed with lower quantum yields. In these experiments the primary excitation was provided at the second-harmonic frequency of a *Q*-switched ruby laser, *i.e.* at 347 nm. The energy and width of the excitation pulse were 40 mJ and 15 ns (FWHM) respectively. The maximum observation period with the double-pulsed xenon flashlamp was 20 μs.

3.3. Sample preparation

The samples were kept in Teflon-stoppered silica cells. Deoxygenation, which is not required for the flash photolysis experiments with PQ^{2+} as an acceptor but is rather crucial with DMTP and PMDI, was achieved in most cases by purging the solutions with argon for at least 15 min.

Acknowledgments

We thank Ing. D. Bebelaar of the Physical Chemistry Department of the University of Amsterdam for making available the ruby laser flash photolysis equipment.

We are grateful to Professor R. Kaptein for communication of his photo-CIDNP data on flavin–NADH prior to publication.

References

1 F. M. Martens, J. W. Verhoeven, R. A. Gase, U. K. Pandit and Th. J. de Boer, *Tetrahedron, 34* (1978) 443.
2 F. M. Martens and J. W. Verhoeven, *Recl. Trav. Chim. Pays-Bas, 100* (1981) 228.
3 A. A. Krasnowsky and G. P. Brin, *Dokl. Akad. Nauk U.S.S.R., 153* (1963) 212; *158* (1964) 225.

4 T. W. Ebbesen, G. Levey and L. K. Patterson, *Nature (London), 298* (1982) 545.
5 E. M. Kosower, A. Teuerstein, H. D. Burrows and A. J. Swallow, *J. Am. Chem. Soc., 100* (1978) 5185.
U. Brühlmann and E. Hayon, *J. Am. Chem. Soc., 96* (1974) 6169.
6 J. Moiroux and P. J. Elving, *J. Am. Chem. Soc., 102* (1980) 6533.
7 A. Ohno, T. Shio, H. Yamamoto and S. Oka, *J. Am. Chem. Soc., 103* (1981) 2041, 2045.
8 P. van Eikeren, P. Kenney and R. Tokmakian, *J. Am. Chem. Soc., 101* (1979) 7402.
9 C. Pac, M. Ihama, M. Yasuda, Y. Miyauchi and H. Sakurai, *J. Am. Chem. Soc., 103* (1981) 6495.
10 P. J. Hore, A. Volbeda, K. Dijkstra and R. Kaptein, *J. Am. Chem. Soc., 104* (1982) 6262.
11 W. J. Blaedel and R. G. Haas, *Anal. Chem., 42* (1970) 918.
12 W. van Gerresheim, C. Kruk and J. W. Verhoeven, *Tetrahedron Lett., 23* (1982) 565, and references cited therein.
13 S. Shinkai, T. Tsuno and O. Manabe, *J. Chem. Soc., Chem. Commun.*, (1982) 592.
14 M. Yamamoto, M. Ohaka, K. Kitagawa, S. Nishimoto and Y. Nishijima, *Chem. Lett.*, (1973) 745.
15 B. H. Bielski and P. C. Chan, *J. Am. Chem. Soc., 102* (1980) 1713.
16 A. A. Krasnovsky and G. P. Brin, *Dokl. Akad. Nauk U.S.S.R., 163* (1965) 761.
17 Y. Ohnishi, M. Kagami and A. Ohno, *Chem. Lett.*, (1975) 125.
18 J. H. Borkent, *Dissertation*, University of Amsterdam, 1976.
19 E. F. Ullman and P. Singh, *J. Am. Chem. Soc., 94* (1972) 5077.
20 Y. Kanaoka, *Acc. Chem. Res., 11* (1978) 407.
21 G. C. Schaefer and K. S. Peters, *J. Am. Chem. Soc., 102* (1980) 7566.
22 K. Wallenfels, W. Ertel and K. Friedrich, *Justus Liebigs Ann. Chem.*, (1973) 1663.
23 G. R. Hays, R. Huis, B. Coleman, D. Clague, J. W. Verhoeven and F. Rob, *J. Am. Chem. Soc., 103* (1981) 5140.
24 L. G. Schroff, A. J. A. van der Weerdt, D. J. H. Staalman, J. W. Verhoeven and Th. J. de Boer, *Tetrahedron Lett.*, (1973) 1649.
L. G. Schroff, R. L. J. Zsom, A. J. A. van der Weerdt, P. I. Schrier, J. P. Geerts, N. M. M. Nibbering, J. W. Verhoeven and Th. J. de Boer, *Recl. Trav. Chim. Pays-Bas, 95* (1976) 89.
25 D. Bebelaar, *Chem. Phys., 3* (1974) 205.